NEOPLASIA
www.neoplasia.com

Volume 11 Number 8 August 2009 pp. 732–742 732

Platelet-Derived Growth Factor-Receptor α Strongly Inhibits Melanoma Growth *In Vitro* and *In Vivo*[1]

Debora Faraone*, Maria Simona Aguzzi†, Gabriele Toietta†, Angelo M. Facchiano‡, Francesco Facchiano§, Alessandra Magenta†, Fabio Martelli†, Silvia Truffa†, Eleonora Cesareo¶, Domenico Ribatti#, Maurizio C. Capogrossi† and Antonio Facchiano†

*Laboratorio Biologia Vascolare e Terapia Genica, Centro Cardiologico Monzino, IRCCS, Milano, Italy; †Laboratorio Patologia Vascolare, Istituto Dermopatico dell'Immacolata, IDI-IRCCS, Roma, Italy; ‡Laboratorio Bioinformatica e Biologia Computazionale, Istituto di Scienza dell'Alimentazione CNR, Avellino, Italy; §Dipartimento Ematologia, Oncologia e Medicina Molecolare, Istituto Superiore di Sanità, Roma, Italy; ¶Laboratorio Ingegneria Tessutale e Fisiopatologia Cutanea, Istituto Dermopatico dell'Immacolata, IDI-IRCCS, Roma, Italy; #Dipartimento Anatomia Umana, Policlinico, Bari, Italy

Abstract

Cutaneous melanoma is the most aggressive skin cancer; it is highly metastatic and responds poorly to current therapies. The expression of platelet-derived growth factor receptors (PDGF-Rs) is reported to be reduced in metastatic melanoma compared with benign nevi or normal skin; we then hypothesized that PDGF-Rα may control growth of melanoma cells. We show here that melanoma cells overexpressing PDGF-Rα respond to serum with a significantly lower proliferation compared with that of controls. Apoptosis, cell cycle arrest, pRb dephosphorylation, and DNA synthesis inhibition were also observed in cells overexpressing PDGF-Rα. Proliferation was rescued by PDGF-Rα inhibitors, allowing to exclude nonspecific toxic effects and indicating that PDGF-Rα mediates autocrine antiproliferation signals in melanoma cells. Accordingly, PDGF-Rα was found to mediate staurosporine cytotoxicity. A protein array–based analysis of the mitogen-activated protein kinase pathway revealed that melanoma cells overexpressing PDGF-Rα show a strong reduction of c-Jun phosphorylated in serine 63 and of protein phosphatase 2A/Bα and a marked increase of p38γ, mitogen-activated protein kinase kinase 3, and signal regulatory protein α1 protein expression. In a mouse model of primary melanoma growth, infection with the Ad-vector overexpressing PDGF-Rα reached a significant 70% inhibition of primary melanoma growth ($P < .001$) and a similar inhibition of tumor angiogenesis. All together, these data demonstrate that PDGF-Rα strongly impairs melanoma growth likely through autocrine mechanisms and indicate a novel endogenous mechanism involved in melanoma control.

Neoplasia (2009) 11, 732–742

Abbreviations: AdCMV.PDGF-Rα, recombinant adenoviral vector expressing human PDGF-Rα and EGFP; AdCMV.EGFP, adenoviral vector expressing EGFP; PI, propidium iodide

Address all correspondence to: Antonio Facchiano, Istituto Dermopatico dell'Immacolata, IDI-IRCCS, Laboratorio Patologia Vascolare, Via Monti di Creta 104, 00167 Rome, Italy. E-mail: a.facchiano@idi.it, antoniofacchiano@yahoo.it

[1]The present work was in part supported by grant RF07ONC-25/3 and by Progetto Oncoproteomica Italia–USA (n. 527B/2A/5) to A.F., (n. 27/B4) to F.F., and by Programma Italia-USA Farmacogenomica oncologica (n. 527/A/3A/5) to A.M.F.

[2]This article refers to supplementary material, which is designated by Figure W1 and is available online at www.neoplasia.com.

Received 1 March 2009; Revised 16 April 2009; Accepted 20 April 2009

DOI 10.1593/neo.09408

Introduction

Platelet-derived growth factor (PDGF) family members mediate several different effects, including the control of development, tissue repair, wound healing, atherosclerosis, stem cells' recruitment, and tumor growth [1,2]. The PDGF family consists of five isoforms (PDGF-AA, PDGF-BB, PDGF-CC, PDGF-DD, and PDGF-AB), showing different binding specificity for PDGF-Rα, PDGF-Rβ, and PDGF-Rαβ [3]. PDGF-Rα and PDGF-Rβ, although sharing evolutionary relationships, have distinct ligand specificity and functions [4,5]. PDGF-Rβ induces cell proliferation and migration in different cell types [4–6], whereas role of PDGF-Rα is more controversial, with proproliferative or antiproliferative effects in different cell types [7–12]. PDGF-Rα expression has been investigated in different pathologic conditions; for instance, autoantibodies activating PDGF-Rα play a key role in scleroderma and systemic sclerosis and in multiple sclerosis lesions. Hedgehog pathway mutations may cause basal cell carcinoma, likely through increased expression of PDGF-Rα, and activating mutations of *PDGF-Rα* gene were identified in gastrointestinal tumors.

Melanoma accounts for approximately 4% of skin cancers but causes approximately 80% of skin cancer deaths. Skin melanoma is therefore one of the most aggressive tumors in humans, and a hundred thousand new melanoma cases are reported every year in western countries. Factors influencing melanoma development include excessive exposure to sunlight, skin type, and genetic predisposition. The complex genetic network controlling melanoma growth and progression has been largely investigated, indicating several effectors involved such as neuroblastoma RAS (NRAS), BRAF, phosphatidylinositol 3-kinase (PI3-K), mitogen-activated protein kinase (MAPK) pathway, and B-cell CLL/lymphoma 2 [13]. Platelet-derived growth factor receptors act through MAPKs, and the expression of PDGF receptors has been found to be decreased in metastatic melanoma compared with those in controls [14], explaining at least in part why specific inhibitors of these receptors have not shown clinical benefits in melanoma treatments [15]. This also suggests that loss of PDGF receptors may represent a way to select more aggressive clones sustaining melanoma progression. Hence, low PDGF-Rα levels may underlie, at least in part, melanoma growth with escape from growth/apoptosis control. Conversely, overexpression of such receptor may be associated with melanoma inhibition. This hypothesis is supported by previously published data reporting that PDGF-Rα mediates strong antiproliferative and antichemotaxis effects on vascular smooth muscle cells and endothelial cells [9,10,12,16]. We therefore investigated autocrine effects of PDGF-Rα expression in human melanoma cells and show in the present study that PDGF-Rα overexpression markedly inhibits melanoma growth, both *in vitro* and *in vivo*.

Materials and Methods

Cell Cultures

Human metastatic melanoma cell lines used were SK-MEL-110 [17] and A375-S2, which were from the American Type Culture Collection (ATCC, Manassas, VA), and 397 MEL, which were kindly provided by Dr S. D'Atri [18]. SK-MEL-110 and A375-S2 were grown in Dulbecco's modified Eagle's medium (DMEM; Hyclone, South Logan, UT), 10% fetal calf serum (FCS; Hyclone). 397 MEL were grown in RPMI 1640 (Sigma-Aldrich, Milan, Italy) and 10% FCS (Hyclone). B16F10 mouse melanoma cells were from the ATCC and were grown in DMEM (Hyclone) and 10% FCS (Hyclone). All media were completed by the addition of glutamine and penicillin-streptomycin (Gibco, Carlsbad, CA). Cells were grown at 37°C with 5% CO_2.

Expression of PDGF-Rα in Human Biopsies

Data sets of the gene expression levels from Affymetrix data obtained from biopsies of human melanoma patients were investigated at the GEO database site (http://www.ncbi.nlm.nih.gov/sites/entrez), namely, data sets GDS1375, GDS1989, GDS2200, and GDS1965. The expression levels of PDGF-Rα and PDGF-Rβ, indicated as rank values, were collected and averaged from all available data points, namely, 17 normal skin biopsies, 22 nevi, and 52 melanoma biopsies.

Cells' Transfection

Cells were transfected with a plasmid coding for human PDGF-Rα (PDGF-Rα) or a dominant-negative form of human PDGF-Rα (DN-PDGF-Rα; gifts from Dr C.H. Heldin, Sweden) or pcDNA3 empty vector (Invitrogen, Carlsbad, CA). Cells were cotransfected with pEGFP-N1 (Clontech, Inc, Mountain View, CA) reporter vector (molar ratio, 3:1). Transfection was performed with Lipofectamine PLUS reagent (Invitrogen) as previously reported [12]. The transfection medium was then replaced with medium ± 10% FCS. Transfection efficiency was checked by green fluorescence and reached 40% in all cases.

Proliferation Assay

SK-MEL-110, A375-S2, and 397 MEL were transfected with PDGF-Rα, DN-PDGF-Rα, or pcDNA3 and were allowed to grow for 24, 48, and 72 hours in medium ± 10% FCS [12]. Cells were then harvested and counted. Neutralizing antibody anti–human PDGF-AA (1 ng/ml; R&D Systems, Minneapolis, MN), soluble recombinant mouse PDGF-Rα/Fc chimera (0.08 μg/ml; R&D Systems), caspase 3 inhibitor (50 μM, z-DEVD-FMK; R&D Systems), or staurosporine (50 nM; Calbiochem, San Diego, CA) were also used.

Procaspase 3 and PDGF-Rα Protein Expression in SK-MEL-110

SK-MEL-110 transfected with PDGF-Rα or pcDNA3 were grown in 10% FCS with or without staurosporine (50 nM). Cells were then lysed. Proteins were analyzed by SDS-PAGE and were transferred to nitrocellulose. Western blot analysis was carried out with anti–procaspase 3 (sc-7148; Santa Cruz Biotechnology, Inc, Santa Cruz, CA), anti–PDGF-Rα (sc-431; Santa Cruz Biotechnology), and anti–β-actin (clone ac-15, Product No. 5441; Sigma-Aldrich) antibodies. Bands' detection was achieved by horseradish peroxidase–conjugated secondary antibody (Pierce, Inc, Rockford, IL) and enhanced chemiluminescence detection system (Amersham Pharmacia Biotech, GE Healthcare Europe GmbH, Milan, Italy) and were quantified with a calibrated imaging densitometer (GS 710; Bio-Rad, Hercules, CA).

TUNEL Assays

SK-MEL-110 (8×10^4) were seeded onto glass coverslips. The following day, cells were transfected with PDGF-Rα or pcDNA3 empty vector. After 24 hours, cells were fixed, permeabilized, and incubated with a TUNEL reaction mixture (Boehringer Mannheim, Corp, Gaithersburg, MD) for cell death *in situ* detection. After washing, cells were incubated with Hoechst solution. Hoechst- and TUNEL-positive nuclei were visualized on a fluorescence microscope (Axioplan; Carl Zeiss, Milan, Italy).

Construction of Adenoviral Vectors

A recombinant adenoviral vector expressing EGFP and human PDGF-Rα (GenBank Accession No. NM_006206; AdCMV.PDGF-Rα) was generated using the Ad-Easy system [19]. An adenoviral vector expressing EGFP alone (AdCMV.EGFP) was also generated as control. Viral titers were estimated by serial dilution on human embryonic kidney 293 cells (ATCC No. CRL-1573) and were expressed as plaque-forming units per milliliter (PFU/ml). Viral stocks did not show replication-competent adenovirus particles, as tested on human lung adenocarcinoma A549 cells (ATCC No. CCL-185). Human SK-MEL-110 or mouse B16F10 melanoma cells were transduced at 10, 30, and 100 multiplicity of infection (MOI) with recombinant AdCMV.PDGF-Rα or AdCMV.EGFP resuspended in serum-free DMEM and were incubated for 90 minutes at 37°C and 5% CO_2. Medium was then replaced with DMEM + 10% FCS for 24, 48, and 72 hours. Cells were counted with a hemacytometer and used for the following *in vitro* and *in vivo* experiments. The infection efficiency reached at least 65% in all cases as assessed by FACS analysis.

Flow Cytometry Analysis

Floating and attached PDGF-Rα– or pcDNA3–transfected cells were harvested, fixed, and treated with RNAse (1 mg/ml) and propidium iodide (PI, 5 μg/ml; Sigma-Aldrich). Analysis of sub-G_1 population was carried out on a Coulter Epics XL flow cytometer (Beckman Coulter, Fullerton, CA) and analyzed with WinMDI software (Joseph Trotter; Scripps Research Institute, La Jolla, CA). SK-MEL-110 were also infected with AdCMV.PDGF-Rα or AdCMV.EGFP, incubated for 10 minutes with 20 μM bromodeoxyuridine (BrdU; Sigma), and fixed. Cell cycle analysis was performed by combined BrdU and PI staining using a Becton Dickinson flow cytometer (Franklin Lakes, NJ) and Cell Quest software (Becton Dickinson) for quantification of BrdU-positive cells [20,21].

Analysis of pRb Phosphorylation Status

After a 48-hour culture, infected cells were lysed [20], and protein concentration was assayed by bicinchoninic acid (BCA) protein assay kit (Pierce). Proteins underwent SDS-PAGE and were transferred onto nitrocellulose. The antibodies used for the detection were anti-tubulin (CP06; Oncogene, Cambridge, MA), anti-pRb (G3-245; BD PharMingen, Becton, Dickinson), anti–hypophosphorylated-pRb (G99-549; BD PharMingen), and anti–PDGF-Rα (sc-431; Santa Cruz Biotechnology).

Protein Microarray for MAPK Pathway Analysis

SK-MEL-110 were infected with AdCMV.EGFP or AdCMV.PDGF-Rα. After 24 hours of starvation, cells were lysed according to the data sheet of the Panorama Antibody Microarray for MAPK and PKC pathways (Sigma). Extracts from controls and treated samples (1 mg/ml) were labeled using Cy3 and Cy5 dyes, respectively, (PA23001 and PA25001; GE Healthcare, Waukesha, WI). Replicates were made with inverted staining (Cy5 and Cy3, respectively). Free dye excess was eliminated by centrifuging at 4000 rpm in SigmaSpin columns (Sigma-Aldrich). Simultaneous expression analysis of members of the MAPK and PKC pathway was then achieved with the Panorama Antibody Microarray Kit (Sigma). This array contains 77 different antibodies against members of the MAPK family and several antibodies against housekeeping proteins, each spotted in duplicate on nitrocellulose-coated glass slides. Only samples with a dye-to-protein molar ratio greater than 2 were applied to the antibody microarray, according to the manufacturer. The hybridized microarray slides were scanned on a ScanArray Gx Microarray Analysis System (Perkin Elmer, Wellesley, MA) with 543 and 633 nm lasers. Data were normalized according to the Lowess method [22] and the manufacturer's recommendation. Ratios of treated *versus* control samples for each spot were computed to estimate the relative fold excess. Modulations lower than two-fold or higher than three-fold *versus* control were then validated by Western blot analysis.

Ex Vivo *and* In Vivo *Primary Melanoma Growth Assay*

Ex vivo and *in vivo* mouse primary melanoma growth assays were carried out as previously reported with modifications [23], according to an accepted animal study protocol. Adult male C57BL/6 mice (Jackson Laboratories, Bar Harbor, ME) were anesthetized by an intraperitoneal injection of 2.5% Avertin (Sigma-Aldrich); in *ex vivo* experiments, mice (17 controls and 17 treated, in three independent experiments) received subcutaneous inoculation in the dorsal skin of 1×10^6 B16F10 cells previously (24 hours) infected with 100 MOI AdCMV.PDGF-Rα or AdCMV.EGFP, dissolved in 50 μl of PBS. For *in vivo* experiments, 1×10^6 uninfected B16F10 cells were injected in the dorsal skin, and 4 days later, mice (14 controls and 14 treated, in two independent experiments) were treated with AdCMV.PDGF-Rα or AdCMV.EGFP inoculation (4.5×10^8 PFU/ml each). Three virus injections (333 μl each) were carried out around the tumor site. Tumors were removed 2 weeks after cell inoculation, weighed, fixed in 4% formalin for 48 hours, and embedded in paraffin. Five-micrometer-thick sections from each sample were obtained and evaluated with a photomicroscope software (Olympus, Tokyo, Japan); digital images were obtained with a high-definition camera with a charge-coupled device. Capillaries were identified with antibodies anti-CD31 (monoclonal antibody 1A10; Dako, Milan, Italy) and anti–factor VIII–related antigen (FVIII-RA, M0616; Dako). Immunodetection was performed with a secondary antibody conjugated with alkaline phosphatase (Dako) and Fast Red as chromogen, followed by hematoxylin counterstaining. Primary antibody was omitted in controls.

Statistical Analysis

All experiments were performed at least three times in duplicates. Standard one-tail Student's *t* test was carried out to evaluate the statistical significance; $P < .05$ was considered to be significant.

Results

Expression of PDGF-Rα Is Reduced in Melanoma Compared with Normal Skin

Previous immunohistochemistry analyses, carried out onto tissue microarrays, show that the expression of PDGF-Rα and β is reduced in melanoma cells compared with benign nevi [14], whereas other studies indicate opposing evidence [24]. Expression of PDGF receptors onto melanoma cells membrane may or may not reflect the biology of such tumor and may also depend on the experimental conditions under evaluation. We analyzed gene expression profiles from four independent studies [25–28] in a total of 55 human melanoma biopsies, 22 benign nevi biopsies, and 17 normal skin biopsies. The analysis revealed 36% reduction of the average level of *PDGF-Rα* gene expression, in melanoma biopsies compared with normal skin ($P < .01$), whereas PDGF-Rβ gene expression did not show a significant change (Figure 1). These data, along with results reported in the literature, provided a rationale to suggest that, at least

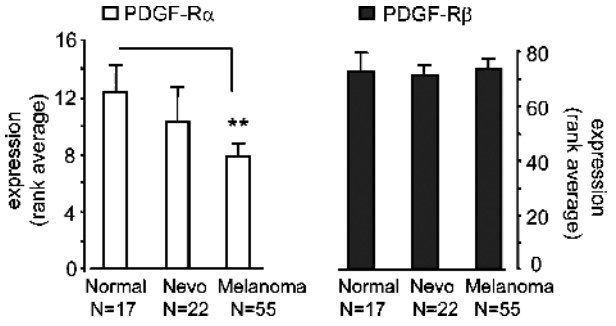

Figure 1. Gene expression level of PDGF-Rα and PDGF-Rβ in human biopsies. Gene expression profiles from healthy skin biopsies, benign nevi biopsies, or malignant melanoma biopsies (i.e., collected and pooled from data sets GDS1375, GDS1989, GDS2200, GDS1965) were retrieved at GEO database site (http://www.ncbi.nlm.nih.gov/sites/entrez). Rank values were collected and averaged. *PDGF-Rα* gene expression is reduced by 36% in melanoma biopsies compared with normal skin (7.9 rank value *vs* 12.4, respectively), whereas PDGF-Rβ expression does not show any significant difference between the groups.

in a significant number of cases, the metastatic potential in melanoma cells may increase in cells showing reduced PDGF-Rα expression, whereas melanoma inhibition may associate with overexpression of such receptor. So far, the action of PDGF-Rs on melanoma cells has been poorly investigated. We therefore investigated the effect of PDGF-Rα and of its ligand PDGF-AA on melanoma growth.

PDGF-Rα Overexpression Inhibits Melanoma Cells Proliferation

Human recombinant PDGF-AA unexpectedly was found to strongly inhibit FCS-induced proliferation of metastatic melanoma cells (SK-MEL-110) in a dose-dependent manner (Figure 2*A*). PDGF-AA binds PDGF-Rα only [3]; therefore, we hypothesized again that this receptor may exert a negative control in melanoma growth. SK-MEL-110 were transfected with an expression plasmid encoding human PDGF-Rα or with a pcDNA3 empty vector as control. Up to three-fold overexpression of PDGF-Rα, by Western blot analysis, was observed at 24 and 48 hours (Figure 2*E*). Transfected melanoma cells proliferated significantly less than controls (transfected with the empty pcDNA3 vector), at 24 and 48 hours, both in the presence and in the absence of FCS (Figure 2, *B* and *C*, respectively). Such antiproliferation effect is reported as representative

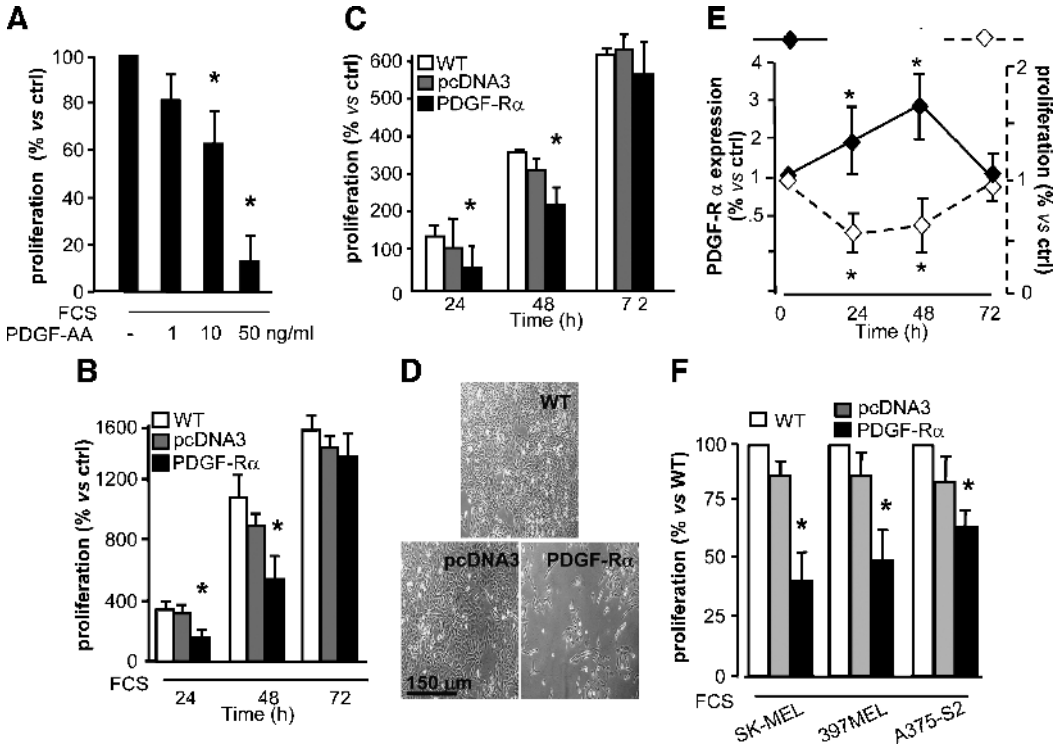

Figure 2. Inhibition of SK-MEL-110 growth. (A) Melanoma cell proliferation is inhibited by PDGF-AA after a 48-hour treatment in 10% FCS (*$P < .05$ *vs* FCS alone): 100% = 11×10^5 cells per well. (B and C) Proliferation (with or without 10% FCS, respectively) of SK-MEL-110 untransfected (WT) or transfected with PDGF-Rα or with pcDNA3 empty vector. Proliferation of cells overexpressing PDGF-Rα was significantly inhibited at 24 and 48 hours of culture. *Bars* indicate mean ± SD of three experiments. Data are percent *versus* number of cells seeded (8×10^4 cells per well). *$P < .05$ *versus* pcDNA3-transfected cells. (D) Representative fields of the experiment depicted in panel B at 48 hours. (E) Inverse relation between proliferation and PDGF-Rα expression. Quantification is reported for PDGF-Rα protein expression by densitometry (left-hand axis) and proliferation (right-hand axis). Data are mean ± SD of three experiments and are expressed as fold induction *versus* control. *$P < .05$ *versus* time 0. (F) At 24 hours, 10% FCS–induced proliferation of human metastatic melanoma cells (SK-MEL-110, A375-S2, and 397 MEL) untransfected (WT) or transfected with PDGF-Rα or with pcDNA3 empty vector. Proliferation was significantly inhibited in cells overexpressing PDGF-Rα. Data are mean ± SD from three experiments. *$P < .05$ *versus* pcDNA3-transfected cells (100% = 326×10^3, 100×10^3, 318×10^3 for SK-MEL-110, 397 MEL, and A375-S2, respectively).

fields in Figure 2*D*. Interestingly, proliferation was inversely related with the expression level of PDGF-Rα as depicted in Figure 2*E*. Transfection with the PDGF-Rα plasmid inhibited the proliferation of two additional human metastatic melanoma cell lines (397 MEL and A375-S2) as well (Figure 2*F*).

These *in vitro* experiments indicated that PDGF-Rα mediates a strong antiproliferative effect in different human melanoma cell lines.

Procaspase 3 Levels and Apoptosis Induction in Melanoma Cells Overexpressing PDGF-Rα

Data reported in Figure 2 suggested that triggering PDGF-Rα with its selective ligand PDGF-AA, or overexpressing PDGF-Rα, induce a marked antiproliferation effect. Figure 3*A* indicates that SK-MEL-110 cells transfected with PDGF-Rα plasmid show a significant reduction in the protein level of procaspase 3, compared with controls, suggesting activation of the apoptosis cascade. According to this hypothesis, TUNEL staining was found in approximately 20% of adherent cells transfected with PDGF-Rα plasmid, whereas it was undetectable in control cells (pcDNA3-transfected cells). Representative fields are reported in Figure 3*B*. Propidium iodide incorporation experiments indicated that PDGF-Rα overexpression also increases the percentage of cells in sub-G_1 phase (Figure W1*A*). The effect onto apoptosis levels was further confirmed in the experiments depicted in Figure 6*A*.

Additional experiments revealed that the antimitogenic effect of PDGF-Rα overexpression is abolished by a specific antibody neutralizing PDGF-AA or by a soluble recombinant PDGF-Rα (srPDGF-Rα) that blocks PDGF-Rα or by z-DEVD-FMK blocking procaspase 3 activation (Figure 3*C*). These data further confirmed that PDGF-Rα inhibits SK-MEL-110 growth with a PDGF-AA–dependent mechanism and a procaspase 3–dependent apoptosis mechanism.

PDGF-Rα Mediates Staurosporine Toxicity

A number of clinical studies indicate a possible effect of staurosporine derivatives in solid tumors, at least in mouse [29,30]. Staurosporine induces apoptosis in melanoma [31] and increases PDGF-Rα expression in myofibroblast [32]. We therefore investigated whether staurosporine cytotoxicity may be associated with PDGF-Rα expression in wild type (i.e., untransfected) melanoma cells. Staurosporine treatment (50 nM) led to a significant increase

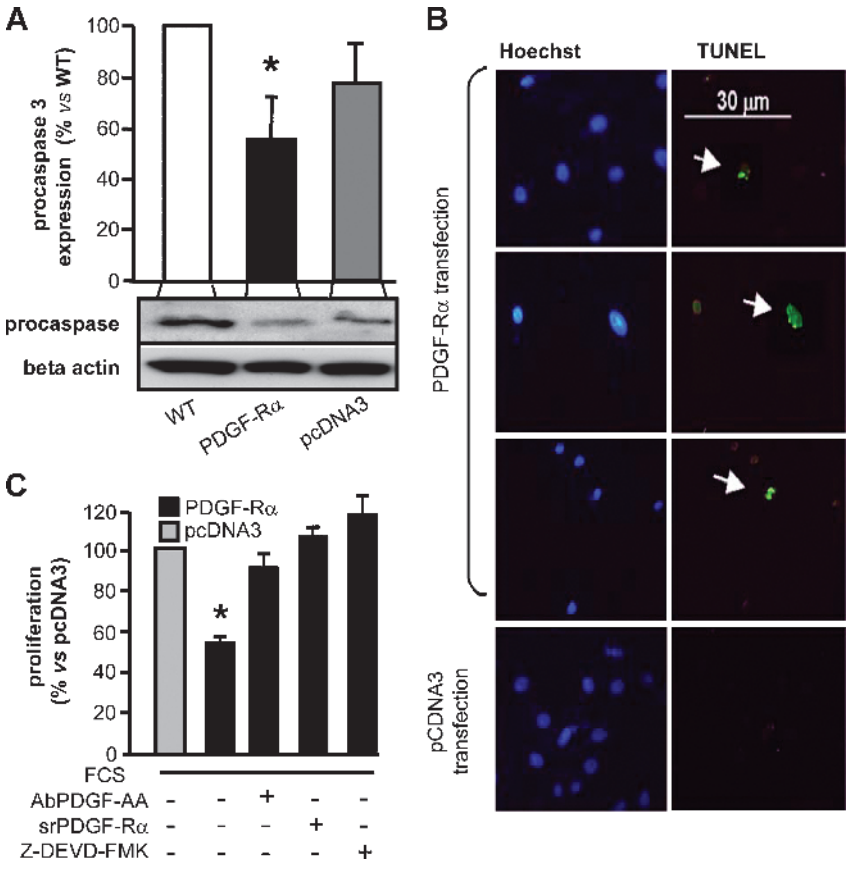

Figure 3. Procaspase 3 protein expression, apoptosis analysis, and PDGF-AA involvement in SK-MEL-110 overexpressing PDGF-Rα. (A) Procaspase 3 protein level was analyzed by Western blot. PDGF-Rα transfection significantly reduced procaspase 3 protein level after 24 hours of culture. *$P < .05$ *versus* pcDNA3-transfected cells. β-Actin was detected to determine protein loading. *Bars* indicate report mean ± SD of three experiments; one representative blot is shown below the bar graphs. (B) Apoptosis of adherent cells transfected with PDGF-Rα after 24 hours of growth. TUNEL staining indicates apoptotic nuclei (arrows) compared with all cells in the field (Hoechst staining). Three fields of cells transfected with PDGF-Rα and one field of control cells are reported. (C) Proliferation of cells transfected with PDGF-Rα plasmid. In the presence of neutralizing antibody to PDGF-AA (AbPDGF-AA) or a srPDGF-Rα or a caspase 3 inhibitor (z-DEVD-FMK), inhibition was completely abolished. Data are mean ± SD of a least three experiments. *$P < .05$ *versus* pcDNA3-transfected cells (100% = 385×10^3).

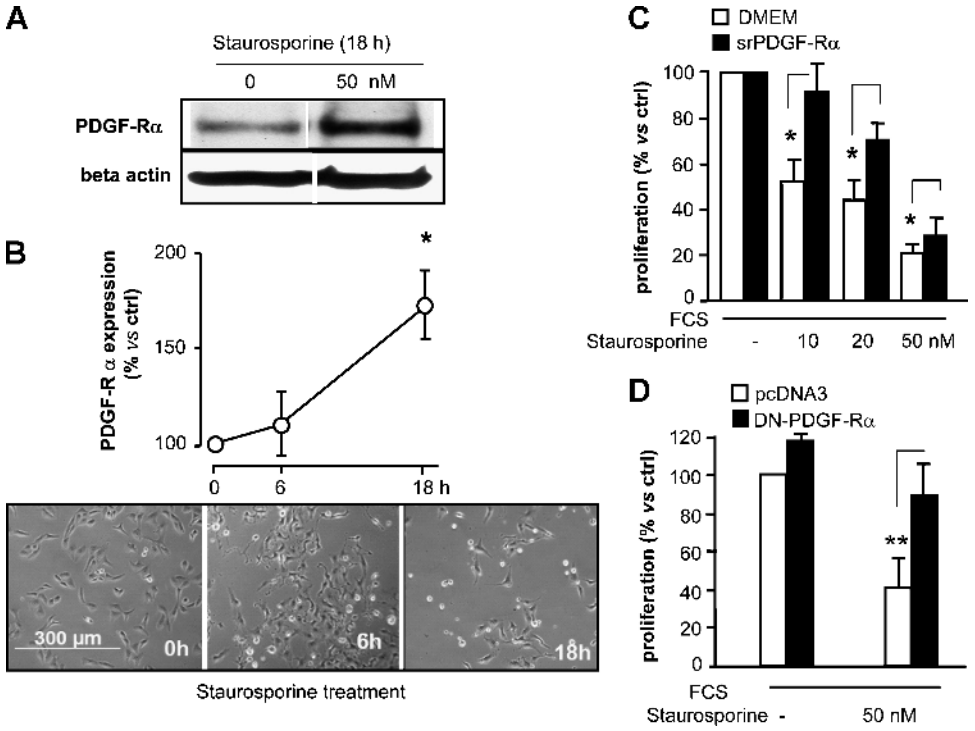

Figure 4. Staurosporine upregulates PDGF-Rα expression in human melanoma cells. (A) SK-MEL-110 cells exposed to 50 nM staurosporine in 10% FCS for 18 hours show increased PDGF-Rα protein expression by Western blot analysis. β-Actin was detected to determine the protein loading. Representative experiment. (B) *Top:* Staurosporine (50 nM) induced a time-dependent increase of PDGF-Rα protein expression. Data are reported as mean ± SD of three experiments. *$P < .05$ *versus* time 0. *Bottom:* One representative image of cells treated with 50 nM staurosporine at 0, 6, and 18 hours in 10% FCS. (C) The 10% FCS–induced proliferation in the presence of staurosporine (0-50 nM). In the presence of srPDGF-Rα, staurosporine cytotoxicity was always significantly reduced. *$P < .05$, white bar *versus* black bar (100% = 540×10^3 and 382×10^3, white bar and black bar respectively). Data are reported as mean ± SD of three experiments. (D) The 10% FCS–induced proliferation was measured in the presence of staurosporine, in pcDNA3- or DN-PDGF-Rα–transfected SK-MEL-110. Staurosporine-induced cytotoxicity was significantly reverted in DN-PDGF-Rα–overexpressing cells. **$P < .001$, white bar *versus* black bar (100% = 247×10^3). Data are reported as mean ± SD of three experiments.

in PDGF-Rα protein levels in a time-dependent manner (Figure 4, *A* and *B*, *upper*). Under such conditions, staurosporine antimitogenic activity followed similar kinetics (Figure 4*B*, *bottom*). PDGF-Rα impairment achieved by treatment with srPDGF-Rα or by transfection with DN-PDGF-Rα significantly reduced staurosporine's effect (Figures 4*C* and 3*D*, respectively), confirming the hypothesis that staurosporine's toxic effects are mediated, at least in part, by PDGF-Rα.

Infection of Melanoma Cells with AdCMV.PDGF-Rα

A recombinant adenoviral vector was generated, expressing EGFP and human PDGF-Rα (AdCMV.PDGF-Rα), to induce an efficient and long-lasting expression of the human *PDGF-Rα* gene. A control adenovirus expressing EGFP only was also generated (AdCMV.EGFP). Cells' transduction achieved an overexpression of at least 10-fold *versus* controls in all cases (Figure 7); transduction efficiency was at least 65% in all experiments. Time course proliferation experiments carried out *in vitro* indicated that infection with 30 MOI of AdCMV.PDGF-Rα markedly reduced or almost abolished proliferation in a dose- and time-dependent way (Figure 5, *A* and *B*).

Mechanisms Triggered by Infection with AdCMV.PDGF-Rα

Cell cycle distribution in cells infected with the AdCMV.PDGF-Rα was monitored by a 10-minute BrdU pulse followed by bivariate FACS analysis of cells stained with PI. DNA synthesis was found to be markedly reduced in PDGF-Rα overexpressing cells compared with control (AdCMV.EGFP–infected cells; 7.4 ± 2.2% *vs* 20.4 ± 2.3%, respectively, after a 48-hour culture, from three independent experiments). Figure 6*A* shows one representative experiment: *top* of the figure reports the BrdU incorporation; *bottom* of the figure shows alteration of cell cycle distribution and increased sub-G_1 population. According to the results reported in Figure 3*B*, cells infected with the AdCMV.PDGF-Rα showed a strong increase in the sub-G_1 population, that is, 14.1 ± 0.35% in AdCMV.PDGF-Rα–infected cells *versus* 0.99 ± 0.27% in AdCMV.EGFP–infected cells (Figure W1*B*).

pRb plays a role in S-phase arrest induced by cytotoxic agents [20,33] and acts as growth suppressor in its hypophosphorylated form [34]. We thus investigated whether PDGF-Rα controls pRb phosphorylation. Two different antibodies, recognizing either all pRb forms or pRb in its hypophosphorylated form only, were used in Western blot analyses. pRb was found mostly in its hyperphosphorylated form in control cells (uninfected and AdCMV.EGFP–infected cells; Figure 6*B*, *lanes 1b and 2b*), whereas a faster migrating hypophosphorylated form appeared in cells overexpressing PDGF-Rα (*lane 3b*) after 48 hours of proliferation. The presence of the pRb hypophosphorylated form was further confirmed using an antibody able to specifically recognize pRb in its hypophosphorylated form (*lane 3c*).

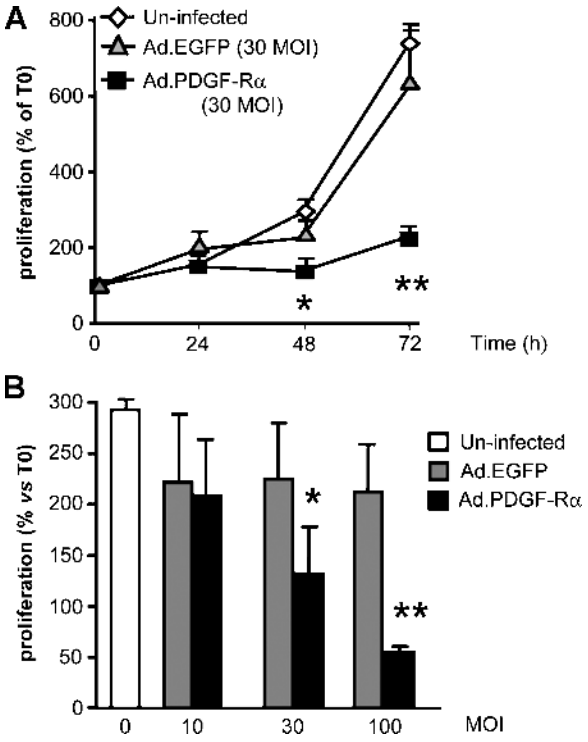

Figure 5. Proliferation of SK-MEL-110 infected with Ad-vector coding for PDGF-Rα. (A) Proliferation of SK-MEL-110 infected with 30 MOI of AdCMV.PDGF-Rα; uninfected cells and AdCMV.EGFP-infected cells were used as control. The 10% FCS–induced proliferation at 24, 48, and 72 hours was almost completely inhibited in AdCMV.PDGF-Rα–infected cells. $*P < .05$, $**P < .01$, *versus* AdCMV.EGFP (cell number at $T = 0$ corresponds to 13×10^5). Data are reported as mean ± SD of three experiments. (B) Dose-dependent effects of 10, 30, and 100 MOI AdCMV.PDGF-Rα infection; 10% FCS–induced proliferation at 48 hours. $*P < .05$, $**P < .01$ *versus* AdCMV.EGFP (cell number at $T = 0$ corresponds to 13×10^5). Data are reported as mean ± SD of three experiments.

All together, these data indicated that PDGF-Rα overexpression induces apoptosis, marked DNA synthesis inhibition, cell cycle alteration, and pRb dephosphorylation, explaining at least in part the observed strong antiproliferative effects.

Molecular Pathways Triggered by PDGF-Rα Overexpression in Melanoma Cells

At least in some cases, melanoma is known to show increased expression levels of MAPK/extracellular regulated kinase (ERK)/JUN signaling pathway members [35] underlying the role MAPK pathway may play in melanoma biology. We therefore investigated, through a protein array–based analysis, the expression of 77 members of the MAPKs pathway in melanoma cells overexpressing PDGF-Rα. The analysis revealed a number of proteins downregulated or upregulated in their expression or phosphorylation status. Namely, phosphorylation of c-Jun at serine 63 (Jun-pS63) and expression of serine/threonine protein phosphatase 2A/B α (PP2A/Bα) isoform were reduced more than two-fold *versus* control (Figure 7, *left-hand side*). Less marked down-regulation of other serine/threonine protein phosphatases' subunits was also observed. On the contrary, expression of p38γ (stress-activated protein kinase 3, SAPK3) isoform was increased more than three-fold *versus* control as well as its upstream kinase MAPK kinase 3 (MKK3) and signal regulatory protein α1 (SIRPα1; Figure 7, *right-hand side*). The expression of other members of the MAPK cascade (i.e., ERK1/2, MEKK4, MAPKK, ERK5, MKK4, MEK, SOS) was not modified. Down-regulation of Jun-pS63 and PP2A/Bα and up-regulation of p38γ and SIRPα1 were then confirmed in a separate Western blot analysis (Figure 7).

Inhibition of Melanoma Growth In Vivo

Such data provided the rationale and mechanistic insights to hypothesize that PDGF-Rα may interfere with melanoma growth *in vivo*. This hypothesis was then tested in a mouse model of primary melanoma growth: in three independent experiments, 17 mice (C57BL/6) were injected with mouse melanoma cells (B16F10) infected with AdCMV.PDGF-Rα (100 MOI) and 17 mice were injected with B16F10 infected with AdCMV.EGFP (100 MOI) as control. Tumors derived from cells infected with AdCMV.PDGF-Rα were markedly smaller in size and weight ($P < .001$) compared with control tumors (Figure 8*A*). The histologic analysis, performed by CD31 staining, revealed a strongly reduced angiogenesis, with a capillary density lowered by at last four-fold (Figure 8*B*); factor VIII staining confirmed these results. This strong effect was confirmed in separate experiments by

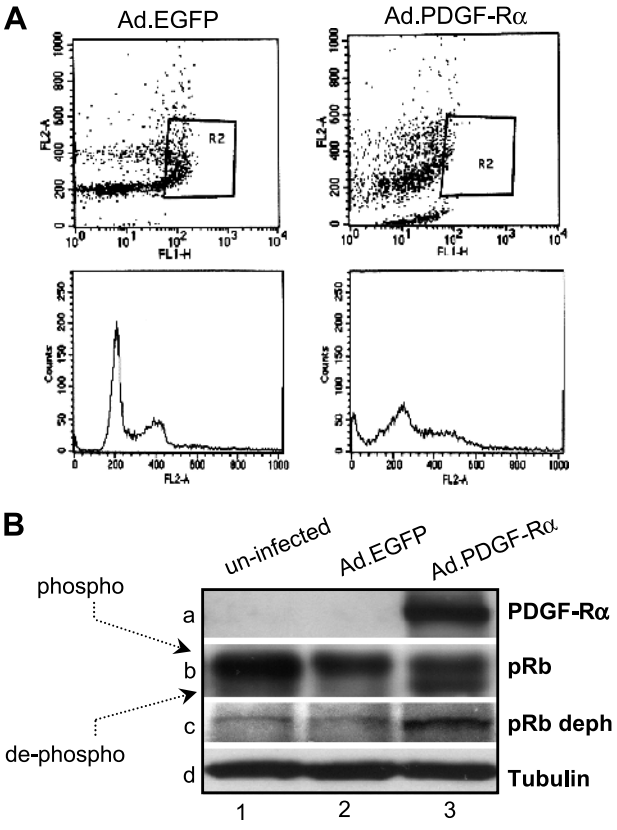

Figure 6. FACS analysis. (A) At 48 hours after AdCMV.PDGF-Rα infection, DNA synthesis is markedly inhibited. A representative image of BrdU incorporation (top) and PI staining (bottom) is shown. (B) SK-MEL-110–uninfected cells (WT) or cells infected with AdCMV.PDGF-Rα or with AdCMV.EGFP were immunoblotted with antibodies to pan-pRb, hypophosphorylated pRb (pRb deph), PDGF-Rα, and tubulin. Cells infected with AdCMV.PDGF-Rα show evident pRb hypophosphorylation (lanes 3b and 3c).

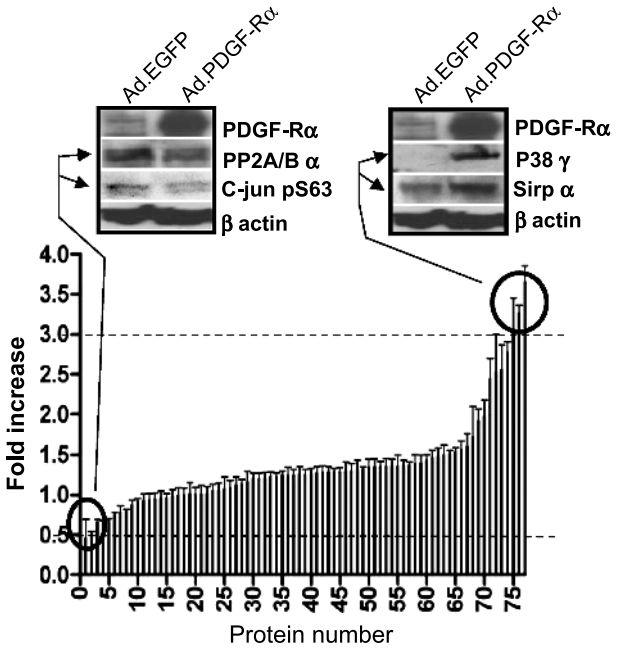

Figure 7. Mitogen-activated protein pathway analysis by protein array. The expression level of 77 members of the MAPK pathway was analyzed and expressed as ratio of cells infected with PDGF-Rα virus *versus* cells infected with EGFP virus. The insets show validation by Western blot analysis. The proteins circled, showing a fold increase or a fold decrease above or below the threshold, respectively, are as follows: 1) phospho c-JUN (pS63); 2) serine/threonine PP2A/Bα; 75) p38 MAPK, nonactivated clone P38-YNP; 76) SIRPα1, MKK3 (SAPKK2, SKK2, MEK3); 77) p38γ (SAPK3). The complete list of proteins numbered from 1 to 77 in the graph is reported as a Supplemental Information. Data are reported as mean ± SD of three experiments.

in vivo local injection of AdCMV.PDGF-Rα or AdCMV.EGFP (4.5×10^8 PFU/ml each) as reported in the Materials and methods section. Four days after injection of normal (i.e., uninfected) melanoma B16F10 cells, 14 mice were treated with local injection of AdCMV.PDGF-Rα in the site of the primary tumor, and a significant reduction of the tumor weight was observed after ten additional days (35% inhibition *vs* control, $P < .05$) compared with 14 mice locally injected with AdCMV.EGFP (Figure 8*C*).

These data indicated that melanoma tumors overexpressing PDGF-Rα show a significantly marked growth inhibition in experiments with either *ex vivo* or *in vivo* treatment.

Discussion

The present study addressed the novel hypothesis that PDGF-Rα may have autocrine inhibitory control on melanoma growth. Such hypothesis derives from several considerations: 1) we previously showed that PDGF-AA and its unique receptor PDGF-Rα exerts a direct antiangiogenic role *in vitro* and *in vivo* [10,12], as opposed to the stimulatory role of PDGF-BB and PDGF-Rβ; 2) other authors reported dual opposing effects of PDGF-Rα and PDGF-Rβ in different cell types [7,8,11,36]; 3) proapoptotic activity of PDGF-AA, the selective ligand of PDGF-Rα, has been reported [37], and a specific down-regulation of PDGF-Rα is necessary to allow *in vitro* growth of human mesothelioma cells [36]; 4) nitric oxide induces apoptosis, and PDGF-Rα is upregulated by nitric oxide donor treatment in renal mesangial cells [38]; 5) interleukin (IL) 1β and staurosporine, known apoptosis inducers in different cell types including melanoma [39], upregulate PDGF-Rα expression [32], suggesting that PDGF-Rα mediates, at least in part, the apoptotic response to these factors; 6) *PDGF-Rα* gene belongs to the growth arrest–specific (*gas*) gene family [40]; and 7) data presented in the current study and by others [14] show that expression of PDGF-Rα is reduced in melanoma compared with normal skin or benign nevi, explaining at least in part why treatment with specific inhibitors of PDGF receptors does not achieve relevant clinical effects in melanoma patients [15] and raising questions on the actual role PDGF receptors play in the control of melanoma progression.

According to these considerations, we hypothesized that melanoma cells expressing low levels of PDGF-Rα may sustain melanoma progression, whereas increased PDGF-Rα may inhibit melanoma.

In the present study, we show that overexpressing PDGF-Rα strongly affects proliferation of four different melanoma cell lines: human SK-MEL-110, A375, 397, and mouse B16. Data reported in the literature indicate A375 and 397 harboring BRAF mutations [41,42], whereas SK-MEL-110 are reported to have wild-type BRAF and wild-type NRAS [43]. Given the effect observed on all tested cell lines, the observed PDGF-Rα–dependent inhibition is more likely to be BRAF/NRAS mutation–independent. PDGF-Rα–forced expression markedly inhibited melanoma growth and associated with procaspase 3 reduction, apoptosis, S-phase reduction, and pRb dephosphorylation. The antiproliferation effect of PDGF-Rα was completely abolished when PDGF-AA or PDGF-Rα was neutralized or when in the presence of caspase 3 inhibitor, further indicating that PDGF-Rα signaling mediates specific inhibitory/apoptotic stimuli in melanoma cells' growth. Staurosporine derivatives such as UCN-01 have shown to potentiate cisplatin anticancer activity and some effect in melanoma patients [44] and in other solid tumors [45]. Hence, the findings that staurosporine modulates PDGF-Rα expression and requires active PDGF-Rα may suggest new ways to increase its clinical efficacy.

The MAPK pathway consists of ERK, Jun N-terminal kinase (JNK), and p38 cascades. The ERK activity is generally required for cell proliferation and transformation, whereas JNK and p38 pathways are involved in stress response. In the present study, the expression level of p38γ (SAPK3) as well as its upstream activator MKK3 (SKK2) were found to be strongly increased in melanoma cells overexpressing PDGF-Rα. p38 mediates melanoma cells death upon nitric oxide donor treatment [46], and p38γ isoform is specifically implicated in melanoma death induced by UV radiation, cisplatin treatment [47], and γ-irradiation–induced cell cycle arrest [48]. The finding that PDGF-Rα overexpression increases p38γ led us to hypothesize that PDGF-Rα in melanoma cells may mediate stressing stimuli leading to growth inhibition, through up-regulation of p38γ and its upstream activator MKK3.

SIRPα1 was also strongly upregulated in melanoma cells overexpressing PDGF-Rα; this was a novel but not surprising finding because SIRPα1 is known to inhibit growth factor–induced cell proliferation, to be activated by PDGF [49], and to exert tumor suppressor activity [50].

c-Jun mediates the transcription response to growth factor and stress, and its selective inhibition has shown promise as antitumor strategy [51]. The concomitant up-regulation of p38γ and down-regulation of c-Jun phosphorylation observed in melanoma cells overexpressing PDGF-Rα may thus represent the signal on different

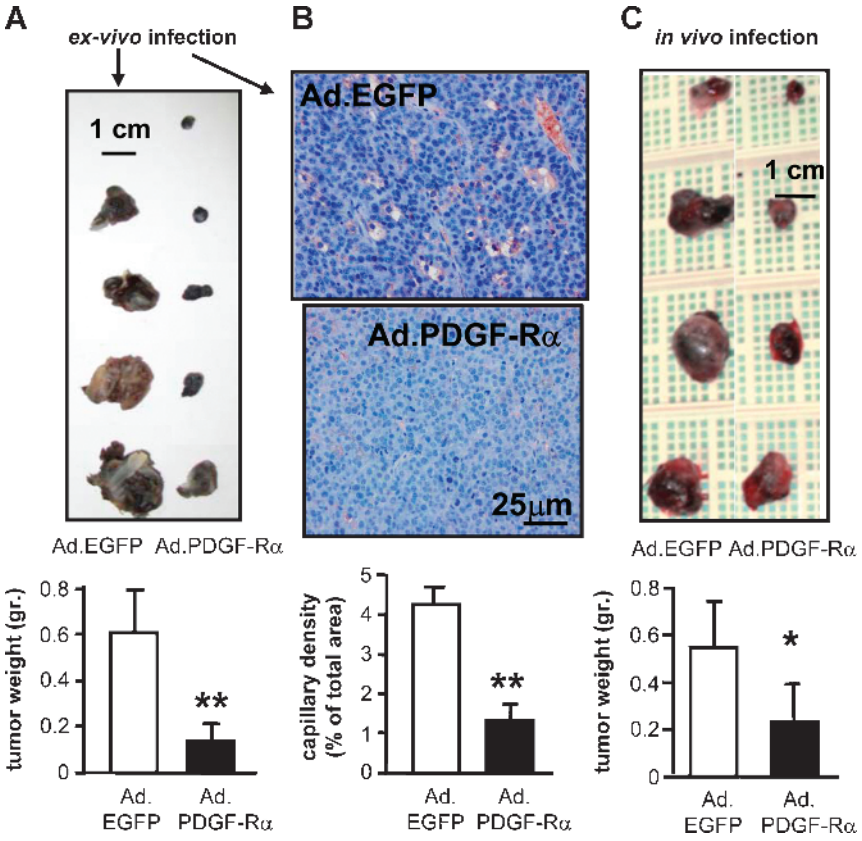

Figure 8. Inhibition of tumor growth in B16F10 melanoma by *ex vivo* and *in vivo* treatment. (A) B16F10 melanoma cells were infected with 100 MOI of AdCMV.PDGF-Rα or AdCMV.EGFP. Tumors obtained were found significantly smaller than controls. *Bars* indicate mean ± SD weight of three different experiments for a total of 17 treated mice and 17 untreated mice. $^{**}P < .001$ *versus* AdCMV.EGFP. (B) Histologic analysis shows a significant reduction of capillaries in tumors derived from cells overexpressing PDGF-Rα *versus* control. CD31 and factor VIII were immunodetected markers of endothelial cells. *Bars* indicate mean ± SD capillary density expressed as percentage of vessels area referred to total area of the slide. $^{**}P < .001$ *versus* AdCMV.EGFP. (C) B16F10 melanoma cells were inoculated in dorsal mice; 4 days later, mice were injected locally with AdCMV.PDGF-Rα or AdCMV.EGFP (4.5×10^8 PFU). Ten days later, tumors were extracted and weighed. Tumors obtained from cells infected with AdCMV.PDGF-Rα were significantly smaller than controls. *Bars* indicate weight ± SD of three different experiments for a total of 14 treated mice and 14 untreated mice. $^{*}P < .03$ *versus* AdCMV.EGFP.

arms of the MAPK pathway, triggering, at least in part, the observed inhibitory effects. Moreover, phosphatase activities are crucial to control protein activation. PP2A is a key multimeric serine/threonine phosphatase. Expression of its B-subunit isoform α was found to be markedly reduced in melanoma cells overexpressing PDGF-Rα, suggesting that, under such conditions, specific substrates of PP2A may not be recognized.

Melanoma is a poor-prognosis cancer in its metastatic phase. Specific tyrosine kinase inhibitors and other receptor inhibitors represent novel promising clinical approaches, with still controversial effects. Although the monoclonal antibody neutralizing vascular endothelial growth factor receptor (bevacizumab) shows some clinical promise, the simultaneous inhibition of PDGF-Rα and PDGF-Rβ has not shown clinical benefit in melanoma [15,52]. These findings raise intriguing questions on the actual role these receptors play in melanoma and may suggest new therapeutic approaches effective at the clinical level. *In vivo* analyses carried out in the present study show that melanoma cells overexpressing PDGF-Rα give rise to tumors markedly smaller in weight and with strongly reduced tumor angiogenesis compared with controls. We speculate that the observed *in vivo* antitumor effect likely derives from the combination of a direct antimitogenic and proapoptotic action on tumor cells on one side and an antiangiogenic activity on the other, likely related to the sequestration of PDGF-Rα ligands. A recently published report found the promitogenic effects of PDGF-CC in melanoma, mediated by PDGF-Rα, through paracrine effects onto fibroblasts and other cell types [53]. All together, these data confirm the different autocrine and paracrine effects of PDGF-Rα.

In conclusion, the current study indicates for the first time a novel role of PDGF-Rα in controlling melanoma cell proliferation and may help understand the mechanisms underlying melanoma's ability to evade apoptosis and drug-induced toxicity.

Acknowledgments

The authors thank Bioinformatics/Proteomics Facility at CNR (Avellino) and Facility for Complex Protein Misture Analysis at the Dipartimento di Ematologia, Oncologia e Medicina Molecolare, ISS (Rome), Italy.

References

[1] Heldin CH and Westermark B (1999). Mechanism of action and *in vivo* role of platelet-derived growth factor. *Physiol Rev* **79**, 1283–1316.

[2] Andrae J, Gallini R, and Betsholtz C (2008). Role of platelet-derived growth factors in physiology and medicine. *Genes Dev* **22**, 1276–1312.

[3] Hoch RV and Soriano P (2003). Roles of PDGF in animal development. *Development* **130**, 4769–4784.

[4] Rosenkranz S and Kazlauskas A (1999). Evidence for distinct signaling properties and biological responses induced by the PDGF receptor alpha and beta subtypes. *Growth Factors* **16**, 201–216.

[5] Klinghoffer RA, Mueting-Nelsen PF, Faerman A, Shani M, and Soriano P (2001). The two PDGF receptors maintain conserved signaling *in vivo* despite divergent embryological functions. *Mol Cell* **7**, 343–354.

[6] Heldin CH, Ostman A, and Ronnstrand L (1998). Signal transduction via platelet-derived growth factor receptors. *Biochim Biophys Acta* **1378**, F79–F113.

[7] Koyama N, Hart CE, and Clowes AW (1994). Different functions of the platelet-derived growth factor-alpha and -beta receptors for the migration and proliferation of cultured baboon smooth muscle cells. *Circ Res* **75**, 682–691.

[8] Clunn GF, Refson JS, Lymn JS, and Hughes AD (1997). Platelet-derived growth factor beta-receptors can both promote and inhibit chemotaxis in human vascular smooth muscle cells. *Arterioscler Thromb Vasc Biol* **17**, 2622–2629.

[9] Facchiano A, De Marchis F, Turchetti E, Facchiano F, Guglielmi M, Denaro A, Palumbo R, Scoccianti M, and Capogrossi MC (2000). The chemotactic and mitogenic effects of platelet-derived growth factor-BB on rat aorta smooth muscle cells are inhibited by basic fibroblast growth factor. *J Cell Sci* **113**, 2855–2863.

[10] De Marchis F, Ribatti D, Giampietri C, Lentini A, Faraone D, Scoccianti M, Capogrossi MC, and Facchiano A (2002). Platelet-derived growth factor inhibits basic fibroblast growth factor angiogenic properties *in vitro* and *in vivo* through its alpha receptor. *Blood* **99**, 2045–2053.

[11] Yu J, Liu XW, and Kim HR (2003). Platelet-derived growth factor (PDGF) receptor-alpha–activated c-Jun NH2-terminal kinase-1 is critical for PDGF-induced $p21^{WAF1/CIP1}$ promoter activity independent of p53. *J Biol Chem* **278**, 49582–49588.

[12] Faraone D, Aguzzi MS, Ragone G, Russo K, Capogrossi MC, and Facchiano A (2006). Heterodimerization of FGF-receptor 1 and PDGF-receptor-alpha: a novel mechanism underlying the inhibitory effect of PDGF-BB on FGF-2 in human cells. *Blood* **107**, 1896–1902.

[13] Hocker TL, Singh MK, and Tsao H (2008). Melanoma genetics and therapeutic approaches in the 21st century: moving from the benchside to the bedside. *J Invest Dermatol* **128**, 2575–2595.

[14] Shen SS, Zhang PS, Eton O, and Prieto VG (2003). Analysis of protein tyrosine kinase expression in melanocytic lesions by tissue array. *J Cutan Pathol* **30**, 539–547.

[15] Wyman K, Atkins MB, Prieto V, Eton O, McDermott DF, Hubbard F, Byrnes C, Sanders K, and Sosman JA (2006). Multicenter Phase II trial of high-dose imatinib mesylate in metastatic melanoma: significant toxicity with no clinical efficacy. *Cancer* **106**, 2005–2011.

[16] Palumbo R, Gaetano C, Antonini A, Pompilio G, Bracco E, Ronnstrand L, Heldin CH, and Capogrossi MC (2002). Different effects of high and low shear stress on platelet-derived growth factor isoform release by endothelial cells: consequences for smooth muscle cell migration. *Arterioscler Thromb Vasc Biol* **22**, 405–411.

[17] Gorospe M, Cirielli C, Wang X, Seth P, Capogrossi MC, and Holbrook NJ (1997). p21(Waf1/Cip1) protects against p53-mediated apoptosis of human melanoma cells. *Oncogene* **14**, 929–935.

[18] Lacal PM, Failla CM, Pagani E, Odorisio T, Schietroma C, Falcinelli S, Zambruno G, and D'Atri S (2000). Human melanoma cells secrete and respond to placenta growth factor and vascular endothelial growth factor. *J Invest Dermatol* **115**, 1000–1007.

[19] He TC, Zhou S, da Costa LT, Yu J, Kinzler KW, and Vogelstein B (1998). A simplified system for generating recombinant adenoviruses. *Proc Natl Acad Sci USA* **95**, 2509–2514.

[20] Cicchillitti L, Fasanaro P, Biglioli P, Capogrossi MC, and Martelli F (2003). Oxidative stress induces protein phosphatase 2A–dependent dephosphorylation of the pocket proteins pRb, p107, and p130. *J Biol Chem* **278**, 19509–19517.

[21] Magenta A, Fasanaro P, Romani S, Di Stefano V, Capogrossi MC, and Martelli F (2008). Protein phosphatase 2A subunit PR70 interacts with pRb and mediates its dephosphorylation. *Mol Cell Biol* **28**, 873–882.

[22] Quackenbush J (2002). Microarray data normalization and transformation. *Nat Genet* **32**, 496–501.

[23] Marcellini M, De Luca N, Riccioni T, Ciucci A, Orecchia A, Lacal PM, Ruffini F, Pesce M, Cianfarani F, Zambruno G, et al. (2006). Increased melanoma growth and metastasis spreading in mice overexpressing placenta growth factor. *Am J Pathol* **169**, 643–654.

[24] McGary EC, Onn A, Mills L, Heimberger A, Eton O, Thomas GW, Shtivelband M, and Bar-Eli M (2004). Imatinib mesylate inhibits platelet-derived growth factor receptor phosphorylation of melanoma cells but does not affect tumorigenicity *in vivo*. *J Invest Dermatol* **122**, 400–405.

[25] Talantov D, Mazumder A, Yu JX, Briggs T, Jiang Y, Backus J, Atkins D, and Wang Y (2005). Novel genes associated with malignant melanoma but not benign melanocytic lesions. *Clin Cancer Res* **11**, 7234–7242.

[26] Smith AP, Hoek K, and Becker D (2005). Whole-genome expression profiling of the melanoma progression pathway reveals marked molecular differences between nevi/melanoma *in situ* and advanced-stage melanomas. *Cancer Biol Ther* **4**, 1018–1029 (E-pub 2005 Sep 1019).

[27] Nindl I, Dang C, Forschner T, Kuban RJ, Meyer T, Sterry W, and Stockfleth E (2006). Identification of differentially expressed genes in cutaneous squamous cell carcinoma by microarray expression profiling. *Mol Cancer* **5**, 30.

[28] Hoek K, Rimm DL, Williams KR, Zhao H, Ariyan S, Lin A, Kluger HM, Berger AJ, Cheng E, Trombetta ES, et al. (2004). Expression profiling reveals novel pathways in the transformation of melanocytes to melanomas. *Cancer Res* **64**, 5270–5282.

[29] Grosios K (2001). UCN-01 Kyowa Hakko Kogyo Co. *Curr Opin Investig Drugs* **2**, 287–297.

[30] Millward MJ, House C, Bowtell D, Webster L, Olver IN, Gore M, Copeman M, Lynch K, Yap A, Wang Y, et al. (2006). The multikinase inhibitor midostaurin (PKC412A) lacks activity in metastatic melanoma: a phase IIA clinical and biologic study. *Br J Cancer* **95**, 829–834.

[31] Zhang XD, Gillespie SK, and Hersey P (2004). Staurosporine induces apoptosis of melanoma by both caspase-dependent and -independent apoptotic pathways. *Mol Cancer Ther* **3**, 187–197.

[32] Lindroos PM, Wang YZ, Rice AB, and Bonner JC (2001). Regulation of PDGFR-alpha in rat pulmonary myofibroblasts by staurosporine. *Am J Physiol Lung Cell Mol Physiol* **280**, L354–L362.

[33] Knudsen KE, Booth D, Naderi S, Sever-Chroneos Z, Fribourg AF, Hunton IC, Feramisco JR, Wang JY, and Knudsen ES (2000). RB-dependent S-phase response to DNA damage. *Mol Cell Biol* **20**, 7751–7763.

[34] Cobrinik D (2005). Pocket proteins and cell cycle control. *Oncogene* **24**, 2796–2809.

[35] Lewis TB, Robison JE, Bastien R, Milash B, Boucher K, Samlowski WE, Leachman SA, Dirk Noyes R, Wittwer CT, Perreard L, et al. (2005). Molecular classification of melanoma using real-time quantitative reverse transcriptase–polymerase chain reaction. *Cancer* **104**, 1678–1686.

[36] Metheny-Barlow LJ, Flynn B, van Gijssel HE, Marrogi A, and Gerwin BI (2001). Paradoxical effects of platelet-derived growth factor-A overexpression in malignant mesothelioma. Antiproliferative effects *in vitro* and tumorigenic stimulation *in vivo*. *Am J Respir Cell Mol Biol* **24**, 694–702.

[37] Kim HR, Upadhyay S, Li G, Palmer KC, and Deuel TF (1995). Platelet-derived growth factor induces apoptosis in growth-arrested murine fibroblasts. *Proc Natl Acad Sci USA* **92**, 9500–9504.

[38] Beck KF, Guder G, Schaefer L, Pleskova M, Babelova A, Behrens MH, Mihalik D, Beck M, Schaefer RM, and Pfeilschifter J (2005). Nitric oxide upregulates induction of PDGF receptor-alpha expression in rat renal mesangial cells and in anti–Thy-1 glomerulonephritis. *J Am Soc Nephrol* **16**, 1948–1957.

[39] Wang C, Wang MW, Tashiro S, Onodera S, and Ikejima T (2005). IL-1beta acts in synergy with endogenous IL-1beta in A375-S2 human melanoma cell apoptosis through mitochondrial pathway. *J Korean Med Sci* **20**, 555–561.

[40] Lih CJ, Cohen SN, Wang C, and Lin-Chao S (1996). The platelet-derived growth factor alpha-receptor is encoded by a growth-arrest–specific (*gas*) gene. *Proc Natl Acad Sci USA* **93**, 4617–4622.

[41] VanBrocklin MW, Verhaegen M, Soengas MS, and Holmen SL (2009). Mitogen-activated protein kinase inhibition induces translocation of Bmf to promote apoptosis in melanoma. *Cancer Res* **69**, 1985–1994.

[42] Eskandarpour M, Kiaii S, Zhu C, Castro J, Sakko AJ, and Hansson J (2005). Suppression of oncogenic NRAS by RNA interference induces apoptosis of human melanoma cells. *Int J Cancer* **115**, 65–73.

[43] Wang YF, Jiang CC, Kiejda KA, Gillespie S, Zhang XD, and Hersey P (2007). Apoptosis induction in human melanoma cells by inhibition of MEK is caspase-independent and mediated by the Bcl-2 family members PUMA, Bim, and Mcl-1. *Clin Cancer Res* **13**, 4934–4942.

[44] Bedikian AY, Plager C, Stewart JR, O'Brian CA, Herdman SK, Ross M, Papadopoulos N, Eton O, Ellerhorst J, and Smith T (2001). Phase II evaluation of bryostatin-1 in metastatic melanoma. *Melanoma Res* **11**, 183–188.

[45] Edelman MJ, Bauer KS Jr, Wu S, Smith R, Bisacia S, and Dancey J (2007). Phase I and pharmacokinetic study of 7-hydroxystaurosporine and carboplatin in advanced solid tumors. *Clin Cancer Res* **13**, 2667–2674.

[46] Maksimovic-Ivanic D, Mijatovic S, Harhaji L, Miljkovic D, Dabideen D, Fan Cheng K, Mangano K, Malaponte G, Al-Abed Y, Libra M, et al. (2008). Anticancer properties of the novel nitric oxide–donating compound (*S*,*R*)-3-

phenyl-4,5-dihydro-5-isoxazole acetic acid–nitric oxide *in vitro* and *in vivo*. *Mol Cancer Ther* **7**, 510–520.

[47] Pillaire MJ, Nebreda AR, and Darbon JM (2000). Cisplatin and UV radiation induce activation of the stress-activated protein kinase p38gamma in human melanoma cells. *Biochem Biophys Res Commun* **278**, 724–728.

[48] Wang X, McGowan CH, Zhao M, He L, Downey JS, Fearns C, Wang Y, Huang S, and Han J (2000). Involvement of the MKK6-p38gamma cascade in gamma-radiation–induced cell cycle arrest. *Mol Cell Biol* **20**, 4543–4552.

[49] Cant CA and Ullrich A (2001). Signal regulation by family conspiracy. *Cell Mol Life Sci* **58**, 117–124.

[50] Yamasaki Y, Ito S, Tsunoda N, Kokuryo T, Hara K, Senga T, Kannagi R, Yamamoto T, Oda K, Nagino M, et al. (2007). SIRPalpha1 and SIRPalpha2: their role as tumor suppressors in breast carcinoma cells. *Biochem Biophys Res Commun* **361**, 7–13.

[51] Zhang G, Dass CR, Sumithran E, Di Girolamo N, Sun LQ, and Khachigian LM (2004). Effect of deoxyribozymes targeting c-Jun on solid tumor growth and angiogenesis in rodents. *J Natl Cancer Inst* **96**, 683–696.

[52] Ugurel S, Hildenbrand R, Zimpfer A, La Rosee P, Paschka P, Sucker A, Keikavoussi P, Becker JC, Rittgen W, Hochhaus A, et al. (2005). Lack of clinical efficacy of imatinib in metastatic melanoma. *Br J Cancer* **92**, 1398–1405.

[53] Anderberg C, Li H, Fredriksson L, Andrae J, Betsholtz C, Li X, Eriksson U, and Pietras K (2009). Paracrine signaling by platelet-derived growth factor-CC promotes tumor growth by recruitment of cancer-associated fibroblasts. *Cancer Res* **69**, 369–378.

Supplemental Information

The complete list of proteins numbered from 1 to 77 in the graph of Figure 7 is the following (see also antibody list at: http://www.sigmaaldrich.com/etc/medialib/docs/Sigma-Aldrich/Bulletin/mpaa3antibodylist.Par.0001.File.tmp/mpaa3antibodylist.pdf): 1) phospho c-JUN (pS63); 2) serine/threonine PP2A/Bα; 3) serine/threonine PP2A/B′ pan 2; 4) serine/threonine PP2A/Bγ; 5) serine/threonine protein phosphatase 1γ1; 6) serine/threonine protein phosphatase 2Cα/β; 7) c-erbB-4 cl.HER4-36; 8) serine/threonine protein phosphatase 1/β; 9) c-erbB-3 cl.RTJ1; 10) serine/threonine PP2A/A; 11) MAPK, activated (diphosphorylated ERK-1 and 2) cl. MAPK-YT; 12) protein kinase Cβ1 cl.PK-B13; 13) MAPK (ERK-1, ERK-2); 14) p38 MAPK, activated diphosphorylated p38 clone P38-TY; 15) c-Jun N-terminal kinase (JNK1, JNK2); 16) vascular endothelial growth factor receptor 1; 17) S6 kinase; 18) MAPK, non-phosphorylated ERK cl.ERK-NP2; 19) c-erbB-2 clone HER2-96; 20) MEKK4 clone MEKK4-338; 21) phosphotyrosine clone pT-154; 22) protein kinase Cα; 23) MAPK kinase (MEK, MAPKK); 24) MAPK, monophosphorylated threonine clone ERK-YNP; 25) Ap-1; 26) MCL-1; 27) phosphatidylinositol 3-kinase (PI3-K, p85α); 28) phosphothreonine clone PTR-8; 29) MAPK kinase 4 (MKK4, SEK1, JNKK1); 30) protein tyrosine phosphatase PEST clone AG25; 31) MAPK, monophosphorylated tyrosine clone ERK-PY193; 32) JNK, activated (diphosphorylated JNK) clone JNK-PT48; 33) Crk-L; 34) GAPDH clone GAPDH-71.1; 35) CRK-II; 36) ATF2; 37) phosphoserine clone PSR-45; 38) MAPK phosphatase 1 (MKP-1); 39) Sos1; 40) protein kinase Cγ clone PK-G4; 41) P130^{cas}; 42) protein kinase Cδ; 43) MAPK (ERK-1); 44) MAPK, activated/monophosphorylated (phosphothreonine ERK-1 and 2) clone ERK-PT115; 45) c-CBL; 46) MAPK activated protein kinase 2 (MAKAPK2); 47) RSK1; 48) p38 MAPK; 49) protein phosphatase 1α; 50) estrogen receptor; 51) ERK5 (big MAPK, BMK1); 52) KSR clone C3H7D2; 53) ATF 1; 54) protein kinase Cβ1; 55) phospho ATF 2 (pThr69,71) clone ATF-22P; 56) SH-PTP2 (SHP-2); 57) ILK; 58) Grb-2 clone GRB-232; 59) RAF1; 60) phospholipase Cγ1 (PLCγ1); 61) RAF1 clone RNP1; 62) protein kinase Cβ2 clone PK-B26; 63) protein kinase Cε; 64) ILK clone 65; 65) epidermal growth factor receptor clone F4; 66) protein kinase C cl.MC5; 67) phospholipase A2; 68) secretory group V cl.MCL-3G1; 69) phospho c-JUN (pS73); 70) protein kinase Cβ2; 71) protein kinase Cζ; 72) MAPK 2 (ERK-2) clone: 1B3B9; 73) protein kinase Cη; 74) protein kinase Cγ; 75) p38 MAPK, nonactivated clone P38-YNP; 76) SIRPα1, MKK3 (SAPKK2, SKK2, MEK3); and 77) p38γ (SAPK3).

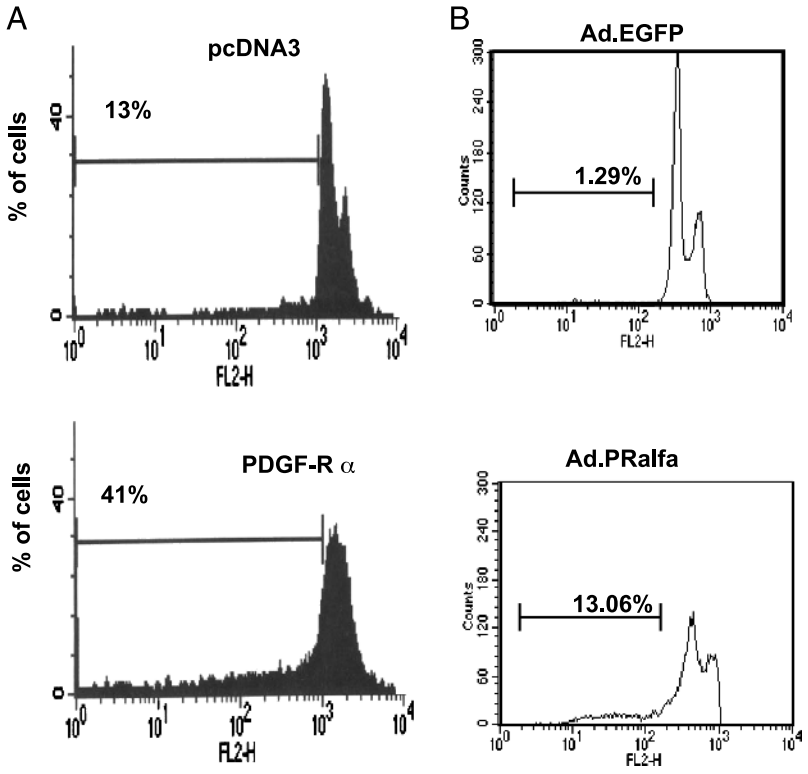

Figure W1. Propidium iodide incorporation analyzed by FACS analysis, in SK-MEL-110 cells transfected with pcDNA3 or PDGF-Rα plasmid (A) or infected with AdCMV.EGFP or AdCMV.PDGF-Rα (B).